Nuclear factor κB–inducing kinase activation as a mechanism of pancreatic β cell failure in obesity

Elisabeth K. Malle,[1] Nathan W. Zammit,[1] Stacey N. Walters,[1] Yen Chin Koay,[8] Jianmin Wu,[2,5] Bernice M. Tan,[1] Jeanette E. Villanueva,[1] Robert Brink,[3,5] Tom Loudovaris,[6] James Cantley,[7] Shelli R. McAlpine,[8] Daniel Hesselson,[4] and Shane T. Grey[1]

[1]Transplantation Immunology Group, Immunology Division, [2]Cancer Bioinformatics, Cancer Division, [3]B Cell Biology, Immunology Division, and [4]Beta Cell Regeneration, Diabetes and Metabolism Division, Garvan Institute of Medical Research, Darlinghurst NSW 2010, Australia
[5]St Vincent's Clinical School, University of New South Wales, Sydney NSW 2010, Australia
[6]St. Vincent's Institute of Medical Research, Fitzroy VIC 3065, Australia
[7]Department of Physiology, Anatomy and Genetics, University of Oxford, Oxford OX1 3PT, England, UK
[8]School of Chemistry, University of New South Wales, Sydney NSW 2052, Australia

The Journal of Experimental Medicine

The nuclear factor κB (NF–κB) pathway is a master regulator of inflammatory processes and is implicated in insulin resistance and pancreatic β cell dysfunction in the metabolic syndrome. Whereas canonical NF–κB signaling is well studied, there is little information on the divergent noncanonical NF–κB pathway in the context of pancreatic islet dysfunction. Here, we demonstrate that pharmacological activation of the noncanonical NF–κB–inducing kinase (NIK) disrupts glucose homeostasis in zebrafish in vivo. We identify NIK as a critical negative regulator of β cell function, as pharmacological NIK activation results in impaired glucose-stimulated insulin secretion in mouse and human islets. NIK levels are elevated in pancreatic islets isolated from diet–induced obese (DIO) mice, which exhibit increased processing of noncanonical NF–κB components p100 to p52, and accumulation of RelB. TNF and receptor activator of NF–κB ligand (RANKL), two ligands associated with diabetes, induce NIK in islets. Mice with constitutive β cell–intrinsic NIK activation present impaired insulin secretion with DIO. NIK activation triggers the noncanonical NF–κB transcriptional network to induce genes identified in human type 2 diabetes genome–wide association studies linked to β cell failure. These studies reveal that NIK contributes a central mechanism for β cell failure in diet–induced obesity.

CORRESPONDENCE
Shane T. Grey:
s.grey@garvan.org.au

Abbreviations used: AP-1, activator protein 1; BIRC2/3, baculoviral IAP repeat-containing proteins 2 and 3; CREB, cAMP response element-binding; DIO, diet-induced obesity; dpf, day postfertilization; GSIS, glucose-stimulated insulin secretion; GTT, glucose tolerance test; GWAS, genome-wide association studies; HFD, high-fat diet; logFC, logarithmic fold change; LTβR, lymphotoxin β receptor; MV1, monovalent 1; NIK, NF–κB–inducing kinase; PDE7B, phosphodiesterase 7b; POD, postoperative day; RANK, receptor activator of NF–κB; RANKL, RANK ligand; SMAC, second mitochondria-derived activator of caspase; T2D, type 2 diabetes; TBK1, TANK-binding kinase; TRAF, TNFR–associated factor.

Inflammation has emerged as a key component of the metabolic syndrome. The canonical NF–κB pathway is a well-studied regulator of inflammatory processes and is heavily implicated in insulin resistance and β cell dysfunction in diabetes. Inhibition of NF–κB improved glucose tolerance in human and animal studies (Yuan et al., 2001; Hundal et al., 2002; Goldfine et al., 2013). The IκB-like kinases IKK-ε and TANK-binding kinase (TBK1) are downstream NF–κB targets involved in driving insulin resistance (Chiang et al., 2009) and blockade of IKK-ε and TBK1 improves metabolic function in obesity (Reilly et al., 2013). Thus, canonical NF–κB is a central molecular pathway in obesity-dependent changes in the metabolic syndrome.

A divergent arm of NF–κB signaling is the noncanonical NF–κB pathway mediated by NF–κB–inducing kinase (NIK), which is activated downstream of TNF receptor (TNFR) family members including TNFR2, receptor activator of NF–κB (RANK), lymphotoxin β receptor (LTβR), or CD40 upon ligand binding (Sun, 2011). NIK levels and hence its activation are controlled by an E3 ligase complex; TNFR–associated factor 2 (TRAF2) recruits the E3 ligases baculoviral IAP repeat-containing proteins 2 and 3 (BIRC2/3), whereas interactions with
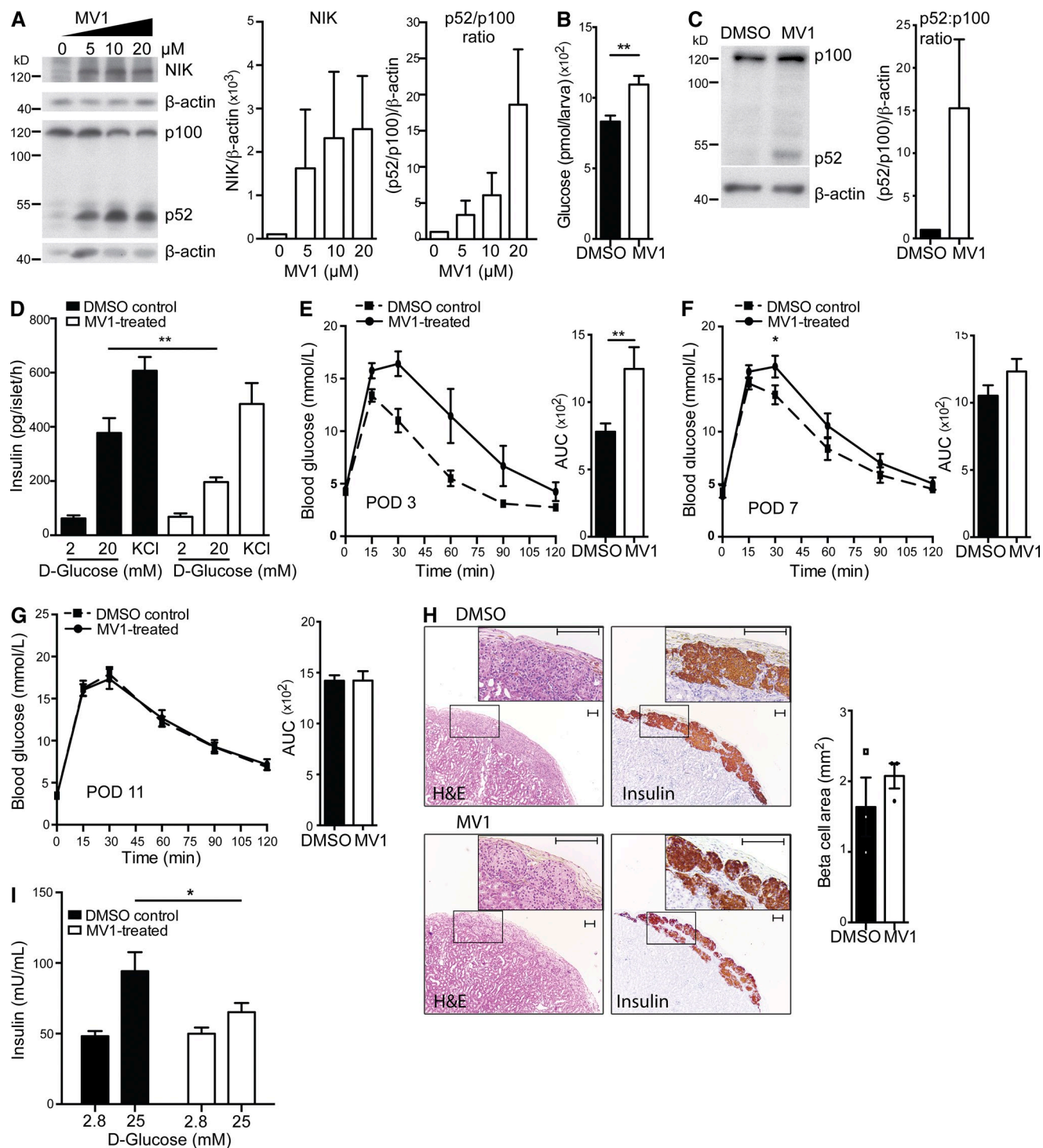
Figure 1. MV1 disrupts glucose homeostasis in zebrafish and impairs β cell function in human and mouse islets. (A) Protein levels of NIK and p100 to p52 processing in the MDA-MB-231/Luc breast cancer cell line treated with increasing concentrations of MV1 were assessed by immunoblotting. A representative of four independent experiments is shown. Histogram data depicts cumulative densitometry relative to β-actin of the four independent experiments. (B) Glucose levels in zebrafish larvae injected with DMSO or MV1 were assessed. The data are mean and SEM derived from seven control and five MV1-treated groups, with four larvae per group, in a representative of two independent experiments. **, P < 0.01. (C) Protein levels of p100 to p52 processing in DMSO and MV1-treated C57BL/6 mouse islets from one islet isolate were assessed by immunoblotting. A representative of three independent experiments is shown. Histogram data depicts cumulative densitometry relative to β-actin of the three independent experiments. (D) In vitro GSIS in 2 and 20 mM D-glucose and in KCl conditions of DMSO control and MV1-treated primary mouse islets was measured. Data are mean and SEM derived from six independent islet isolates for each group, and are representative of two independent experiments. **, P < 0.01. (E–G) Blood glucose and AUC were

TRAF3 allows delivery of NIK to the complex (Vallabhapurapu et al., 2008; Zarnegar et al., 2008). In the absence of a ligand, NIK is ubiquitinated by this complex and targeted for proteasome-dependent degradation, thereby silencing the noncanonical NF-κB pathway (Vallabhapurapu et al., 2008; Zarnegar et al., 2008). The noncanonical NF-κB dimer regulates gene expression through binding to general, as well as specific, noncanonical κB target sites (Bonizzi et al., 2004); however, its targets and the phenotypic consequence of its activation are incompletely known. Studies show that noncanonical NF-κB pathway activation mediated through loss of TRAF2 or TRAF3 promotes expansion of B cells (Gardam et al., 2008), and leads to a shift in the proportions of specific T cell subpopulations (Xie et al., 2011). Recently, activation of the noncanonical NF-κB pathway has been linked to the metabolic syndrome (Choudhary et al., 2011; Sheng et al., 2012; Kiechl et al., 2013). For example, NIK levels are high in muscle biopsies of obese patients, but decline after gastric bypass surgery, weight loss, and a decrease in insulin resistance (Choudhary et al., 2011).

Emerging evidence emphasizes a crucial role for pancreatic β cell dysfunction in type 2 diabetes (T2D). Genome-wide association studies (GWAS) have identified a large number of loci associated with β cell function and survival (Florez, 2008; Guan et al., 2008; Taneera et al., 2012). Further, hyperglycemia (Donath et al., 1999), circulating inflammatory factors (Spranger et al., 2003), or amyloid production in the islet (Verchere et al., 1996) are deleterious for islets and contribute to T2D pathogenesis. This is indicated by diminished β cell mass (Butler et al., 2003), but also by reduced β cell secretory function in T2D patients (Ferrannini and Mari, 2014). Thus, β cell dysfunction in diabetes pathogenesis is now being acknowledged as a critical and major contributor in diabetes pathogenesis. However, the mechanisms for loss of β cell function and mass are incompletely known. Therefore, it is essential to elucidate factors that contribute to both insulin resistance in peripheral tissue and β cell failure.

Core components of the noncanonical NF-κB pathway have been identified in pancreatic islets (Ortis et al., 2010); however, the functional consequence of NIK and subsequent noncanonical NF-κB activation in β cells is completely unknown. We demonstrate here that pharmacologically induced NIK disrupts glucose homeostasis in vivo in a zebrafish model and impairs glucose-stimulated insulin secretion in mouse and human islets. Additionally, a high-fat diet triggers β cell–intrinsic NIK activation and disruption of the E3 ligase control circuit

regulating NIK impairs β cell insulin secretory capacity in a diet-induced obesity model in mice. Here, for the first time, we demonstrate a novel function for NIK and subsequent noncanonical NF-κB activation as a negative regulator of pancreatic β cell function, impairing insulin secretion in diet-induced obesity. NIK activation in the metabolic syndrome is a feature of pancreatic β cells but also insulin-dependent peripheral tissues, thereby providing a tissue-spanning mechanism to link inflammation with multiple tissue failure in diabetes pathogenesis.

RESULTS

Systemic monovalent 1 (MV1) administration impairs glucose homeostasis in zebrafish in vivo

Aberrant BIRC function has been associated with many human cancers (Fulda and Vucic, 2012), leading to the development of a group of peptide-derived drugs called second mitochondria-derived activator of caspase (SMAC) mimetics, which induce the degradation of BIRC2 and BIRC3, thereby interfering with their ability to inhibit apoptosis (Varfolomeev et al., 2007). Concomitantly, degradation of BIRC2 and BIRC3 elicits NIK accumulation, which leads to proteasome-dependent processing of p100 into p52 and hence activates the noncanonical NF-κB pathway (Varfolomeev et al., 2007).

To test whether systemic elevation of NIK mediated by the SMAC mimetic MV1 would alter glucose homeostasis in vivo, we used a zebrafish model. The main organs required for metabolic control, such as the pancreas, islet, and insulin-sensitive tissue (muscle, liver) are conserved in zebrafish, rendering it an excellent model to study glucose homeostasis (Hesselson et al., 2009; Jurczyk et al., 2011; Seth et al., 2013). First, we showed that synthesized MV1 could induce NIK accumulation and processing of p100 into p52 in MDA-MB-231/Luc breast cancer cells, indicating activation of noncanonical NF-κB signaling (Fig. 1 A), as described previously (Varfolomeev et al., 2007). We next injected MV1 into zebrafish larvae at 6 d postfertilization (dpf) and examined glucose levels after 6 h. WT larvae treated with MV1 exhibited increased glucose levels compared with vehicle (DMSO) controls (Fig. 1 B). This indicates that MV1-induced NIK activation disrupts glucose homeostasis in vivo in WT zebrafish.

MV1 administration activates NIK in mouse and human islets and impairs glucose–stimulated insulin secretion

To elucidate whether the defect in glucose homeostasis relates to MV1-induced, NIK-mediated β cell dysfunction, we

---

determined in DMSO control and MV1-treated mouse islet C57BL/6 transplant recipients after i.p. injection of D-glucose at (E) POD 3 (AUC, **, $P < 0.01$; control, $n = 9$; MV1, $n = 8$), (F) POD 7 (*, $P < 0.05$; control, $n = 12$; MV1, $n = 13$), and (G) POD 11 (n.s.; control, $n = 10$; MV1, $n = 10$). Data are representative of three independent mouse cohorts tested. (H) H&E staining and insulin immunostaining of DMSO control and MV1-treated mouse islet grafts are shown. Graft β cell area was determined for three DMSO and three MV1-treated islet grafts by quantification of insulin-positive area in continuous serial graft sections. A representative image for each condition is shown. Boxed insets represent magnified area. Differences in graft area are not significant. *, $P > 0.05$. Bar, 100 µm. (I) In vitro GSIS in 2.8 and 25 mM D-glucose conditions of DMSO control and MV1-treated primary human islets was measured. Data are mean and SEM derived from quintuplets for DMSO and MV1-treated islets and are representative of three independent human islet isolates. *, $P < 0.05$. All data are represented as mean ± SEM; p-values were determined using Student's t test.
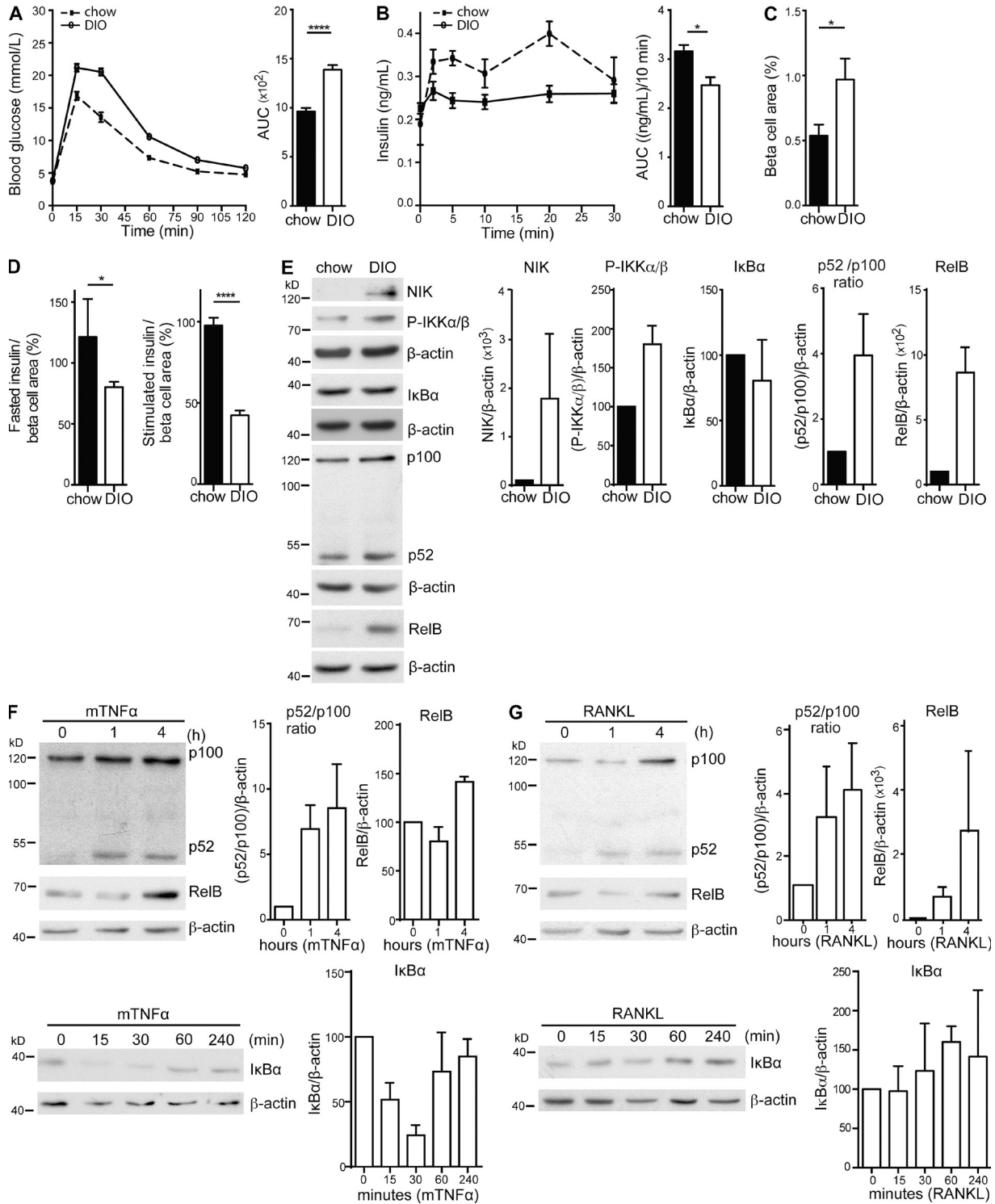
Figure 2. **Pancreatic islets in a DIO model exhibit NIK hyperactivation and display a net β cell secretory defect.** (A) Blood glucose and AUC were determined in 12 chow (dotted line) and 15 DIO (solid line) fed C57BL/6 WT mice (16 wk old) after i.p. injection of D-glucose. Data are representative of three independent mouse cohorts tested. ****, $P < 0.0001$. (B) Insulin levels and AUC (10 min after injection) were determined for 5 chow (dotted line) and 15 DIO (solid line) fed C57BL/6 WT mice (16 wk old) after i.v. injection of D-glucose. Data are representative of three independent mouse cohorts tested. *, $P < 0.05$. (C) Total β cell area was determined for 5 chow- and 5 HFD-fed WT mice by quantification of insulin-positive area in serial graft sections as a percentage of total pancreatic exocrine area (*, $P < 0.05$). (D) Data are mean and SEM showing percentage of net insulin secretion normalized to mean β cell area determined for mice in C. (left) Net fasted insulin levels; (right) net secretion (AUC) for 10 min after D-glucose injection. *, $P < 0.05$; ****, $P < 0.0001$. (E) Protein levels of NIK, IKKα/β phosphorylation, IκBα, p100 to p52 processing, and RelB in one islet isolate from a chow-fed and a DIO

examined the effect of MV1 on insulin secretion of primary C57BL/6 WT islets. Addition of MV1 to WT islets triggered p100 to p52 processing, indicating NIK activation (Fig. 1 C). MV1 had no effect on islet survival in 24-h in vitro cultures as assessed by calcein-AM uptake and ethidium homodimer DNA intercalation (unpublished data). In a glucose-stimulated insulin secretion (GSIS) assay, MV1-treated islets exhibited normal basal insulin output, but insulin secretion was reduced by ∼50% compared with controls when challenged with 20 mM glucose. Potassium chloride (KCl)–stimulated secretion was normal, indicating normal insulin content (Fig. 1 D). To assess the effect of MV1-treatment in vivo, we transplanted either MV1- or vehicle-treated islets into diabetic syngeneic recipients. A glucose tolerance test (GTT) at post-operative day (POD) 3 revealed that, compared with controls, MV1-treated grafts exhibited impaired glucose tolerance (Fig. 1 E). Glucose tolerance was still slightly impaired at POD 7, but had completely resolved by POD 11 such that MV1-treated islets provided equivalent metabolic control to vehicle treated islets (Fig. 1, F and G). Further, MV1-treated grafts exhibited normal morphology and insulin staining, as well as equivalent graft area determined by morphometry (Fig. 1 H). This indicates that acute activation of NIK results in a temporary β cell defect that is reversed upon drug-clearance and suppression of NIK.

NIK activation impairs glucose–stimulated insulin secretion in human islets

We next assessed whether β cell–intrinsic activation of NIK would impair the function of human islets. Human islets treated with MV1 showed normal basal (2.8 mM) but defective glucose-stimulated (25 mM) insulin secretion (Fig. 1 I). Thus, activation of NIK in human islets resulted in impaired β cell function. These data highlight the importance of the NIK pathway and its contribution to β cell dysfunction in human islet physiology.

NIK is activated in islets in diet–induced obesity

To elucidate whether NIK plays a role in islets in a model of glucose intolerance, a diet-induced obesity (DIO) model, C57BL/6 mice were placed on a 45% kcal high-fat diet (HFD). After 8 wk of HFD, these mice showed impaired glucose tolerance and insulin secretion (Fig. 2, A and B), increased β cell mass (Fig. 2 C), and reduced insulin output capacity in fasted conditions and in response to an in vivo glucose challenge (Fig. 2 D). These results are supported by previous studies (Winzell and Ahrén, 2004; Peyot et al., 2010). Islets from DIO mice exhibited activation of the noncanonical NF-κB pathway (Fig. 2 E), as indicated by the accumulation of NIK

and increased phosphorylation of the NIK downstream target IκB kinase α (IKKα). Activated phospho-IKKα phosphorylates NF-κB p100, leading to its proteasome-dependent cleavage releasing active p52. Islets from DIO mice exhibited a higher processing rate of NF-κB p100 to p52 and increased levels of the p52 binding partner RelB, compared with islets from chow-fed controls. As the antibody for Phospho-IKK not only identifies phospho-IKKα but also phospho-IKKβ, we probed for IKKβ downstream target IκBα, which is the canonical NF-κB inhibitor; IκBα levels were normal, indicating absence of canonical NF-κB activation in DIO islets.

TNF and RANKL trigger NIK activation in primary islets

Both TNF and receptor activator of NF-κB ligand (RANKL) activate the noncanonical NF-κB pathway in various cell types, including immune cells (Rauert et al., 2010) and osteoclasts (Novack et al., 2003), and high circulating serum levels of TNF and RANKL are associated with diabetes (Hotamisligil et al., 1995; Kiechl et al., 2013). The effect of TNF and RANKL on noncanonical NF-κB signaling in islets is unknown. TNF induced p100 to p52 processing and RelB accumulation in primary mouse islets, indicating NIK activation (Fig. 2 F). TNF also induced canonical NF-κB activation as shown by degradation of its inhibitor IκBα. RANKL induced p100 to 52 processing and RelB accumulation in primary islets, indicating NIK activation, but did not activate canonical NF-κB signaling (Fig. 2 G). Therefore, both TNF and RANKL activate NIK signaling in primary mouse islets. Additionally, islets isolated from HFD-fed mice show cell-intrinsic activation of NIK and activation of the noncanonical NF-κB pathway with reduced insulin secretion.

Cell–intrinsic NIK activation negatively regulates β cell function in a model of diet–induced obesity

The aforementioned data present a causal link between β cell dysfunction and NIK activation in DIO. To test this concept further, we used a genetic approach whereby β cells would express high levels of active NIK in a cell-intrinsic manner. NIK levels, and hence its activation, are controlled by an E3 ligase complex; TRAF2 recruits the E3 ligases BIRC2/3 while interactions with TRAF3 allow delivery of NIK to the complex (Vallabhapurapu et al., 2008; Zarnegar et al., 2008). In absence of a ligand, NIK is ubiquitinated by this complex and targeted for proteasome-dependent degradation thereby silencing the noncanonical NF-κB pathway (Vallabhapurapu et al., 2008; Zarnegar et al., 2008). Deletion of any one component, i.e., TRAF2, TRAF3, or the BIRC proteins, results in cell-intrinsic hyperactivation of noncanonical NF-κB pathway at a physiological level (Gardam et al., 2008; Zarnegar et al., 2008).

C57BL/6 WT mouse were assessed by immunoblotting. A representative of four independent experiments is shown. Histogram data depict cumulative densitometry relative to β-actin of the four independent experiments. (F and G) Protein levels of p100 to p52 processing and RelB in one (F) TNF- and (G) RANKL-stimulated mouse islet isolate at 0, 1, and 4 h after stimulation. IκBα levels at 0, 15, 30, 60, and 240 min after stimulation were assessed by immunoblotting. A representative of four independent experiments is shown. Histogram data shows cumulative densitometry relative to β-actin of the four independent experiments. All data are represented as mean ± SEM; p-values were determined using Student's *t* test.
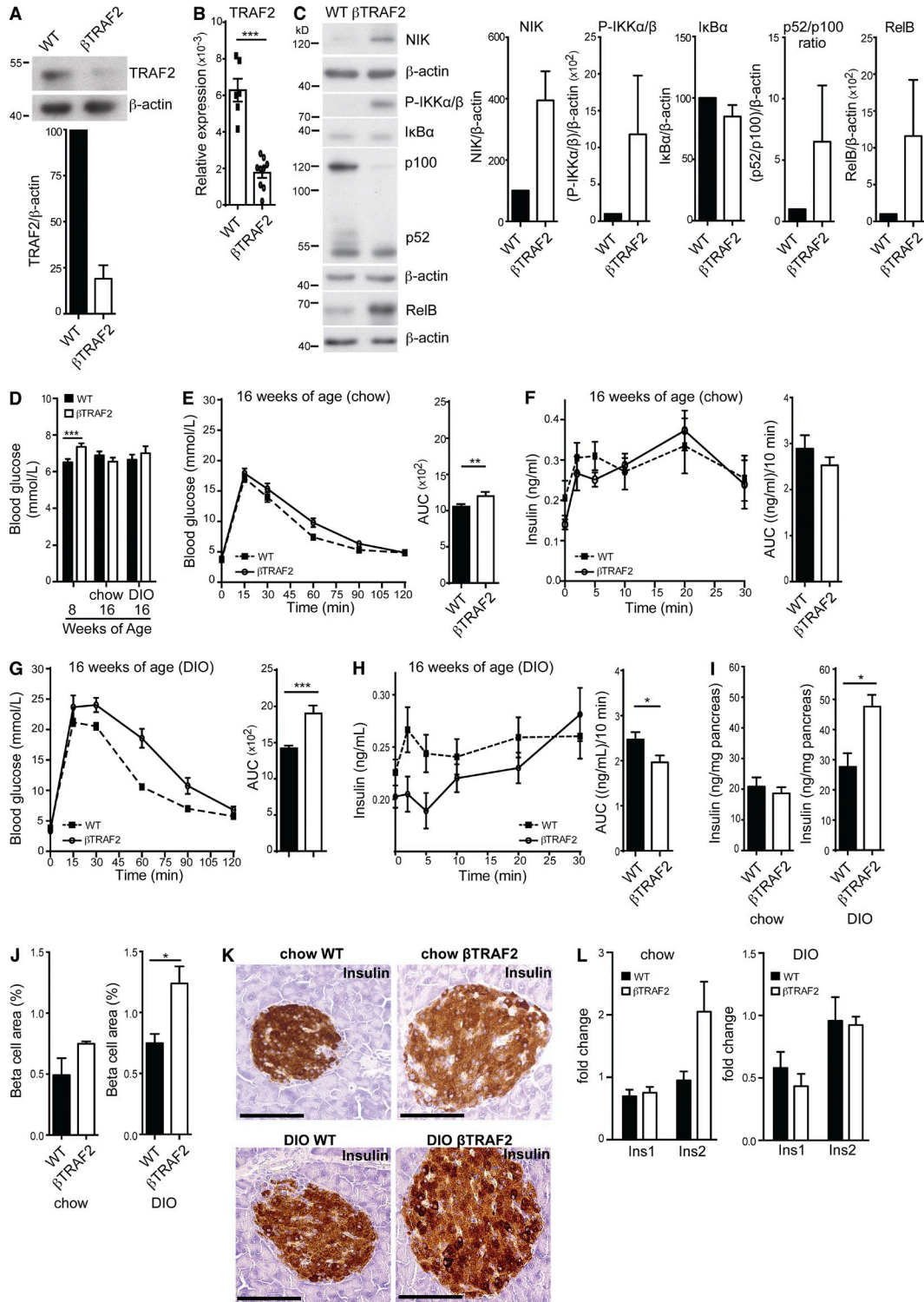
Figure 3. Constitutive NIK activation elicits a defect in insulin secretion. (A) TRAF2 protein levels in WT and βTRAF2 islets isolated from one WT and one βTRAF2 mouse assessed by immunoblotting. A representative of three independent islet isolates tested per genotype is shown. Histogram data depicts mean and SEM cumulative densitometry data relative to β-actin of the three independent experiments. (B) Relative expression of islet TRAF2 mRNA from six WT and nine βTRAF2 islet isolates was determined by RT-PCR. Data are representative of two independent experiments. ***, P < 0.001. (C) Protein levels of NIK, IKKα/β phosphorylation, IκBα, p100 to p52 processing, and RelB in one nonstimulated WT and one βTRAF2 islet isolate were assessed by immunoblotting. A representative of three independent experiments is shown. Histogram data depicts cumulative densitometry relative to β-actin of the three independent experiments. (D) Non-fasted blood glucose levels were determined in 30 TRAF2$_{loxP/loxP}$ (WT), 10 RI Cre (WT), and 24 βTRAF2

To examine how β cell–intrinsic NIK activation would affect glucose homeostasis, we generated β cell–specific TRAF2 knockout (βTRAF2) mice. TRAF2$_{loxP/loxP}$ were crossed with mice expressing Cre under the control of the rat insulin promoter (RIP Cre). TRAF2 mRNA and protein were expressed in TRAF2$_{loxP/loxP}$ islets but depleted in islets from βTRAF2 mice (Fig. 3, A and B). βTRAF2 islets showed high cell-intrinsic accumulation of NIK with hyper-phosphorylation of IKKα (Fig. 3 C). βTRAF2 islets exhibited increased p100 processing into p52 and higher levels of RelB. In contrast, IκBα levels were not changed in βTRAF2 islets, indicating that IKKβ and canonical NF-κB signaling were not activated. Thus, loss of TRAF2 results in cell-intrinsic constitutive activation of NIK in pancreatic β cells.

Chow-fed βTRAF2 mice exhibited normal weight gain over the experimental period of 8 wk and normal glucose tolerance at 8 wk of age (not depicted). They also had mildly elevated nonfasted blood glucose levels (Fig. 3 D) compared with floxed littermates and RIP Cre/+ controls. By 16 wk of age, chow-fed βTRAF2 mice showed very mild glucose intolerance (Fig. 3 E) and no significant difference in insulin secretion (Fig. 3 F) compared with WT mice. However, in a DIO model, βTRAF2 mice showed greatly exacerbated glucose intolerance compared with WT mice (Fig. 3 G). We next examined in vivo insulin secretion (i.v. GTT) to test whether this related to a β cell defect. In this experiment, DIO βTRAF2 mice exhibited a reduction in first-phase insulin secretion (Fig. 3 H). These data demonstrate that β cell–intrinsic activation of NIK results in impaired glucose tolerance due to reduced β cell function.

NIK activation influences β cell mass in a model diet–induced obesity

To determine whether the reduction in insulin secretion was due to decline in insulin production, we determined total pancreatic insulin content and β cell area. On a chow diet, pancreata from βTRAF2 mice showed similar total insulin content as WT mice and normal β cell area (Fig. 3,

I and J). However, in the DIO model, βTRAF2 mice exhibited increased pancreatic insulin content compared with WT mice (Fig. 3 I). This is accompanied by an increase in β cell area in DIO βTRAF2 mice (Fig. 3 J). Also, β cells in βTRAF2 islets exhibited robust insulin expression as determined by insulin immunostaining (Fig. 3 K) and normal levels of *Insulin-1* and *Insulin-2* determined by RT-PCR (Fig. 3 L). Thus, we can conclude that β cell–intrinsic NIK activation results in a loss of insulin secretory capacity rather than a defect in insulin production. Additionally, we hypothesize that the increased β cell mass in DIO βTRAF2 mice most likely represents a physiological compensatory response to the reduced insulin secretory capacity of the βTRAF2 islet.

The function of βTRAF2 islets is impaired after transplantation

In the DIO model, βTRAF2 mice presented a blunted first-phase insulin secretion compared with controls. A subset of transgenic RIP Cre mouse lines have been reported to exhibit hypothalamic Cre expression (Wicksteed et al., 2010). To discern between hypothalamus-mediated and islet-specific defects, we isolated pancreatic βTRAF2 and control islets, and transplanted 150 islet equivalents into streptozotocin-treated diabetic syngeneic C57BL/6 recipients. Under these conditions both WT and βTRAF2 islet grafts restored normal metabolic control (Fig. 4 A). To test β cell function, we performed an i.p. GTT at POD 11. Compared with mice receiving WT islet grafts, βTRAF2 graft recipients exhibited impaired glucose tolerance (Fig. 4 B). Next, we determined insulin secretion in graft recipients via an i.v. GTT at POD 21. Recipients of βTRAF2 islet grafts exhibited a blunted first-phase insulin secretion compared with mice receiving WT islet grafts (Fig. 4 C). Graft pathology revealed that βTRAF2 grafts exhibited normal morphology and insulin staining, as well as equivalent graft area determined by morphometry (Fig. 4 D). Therefore, we conclude that loss of glucose tolerance was not due to β cell loss.
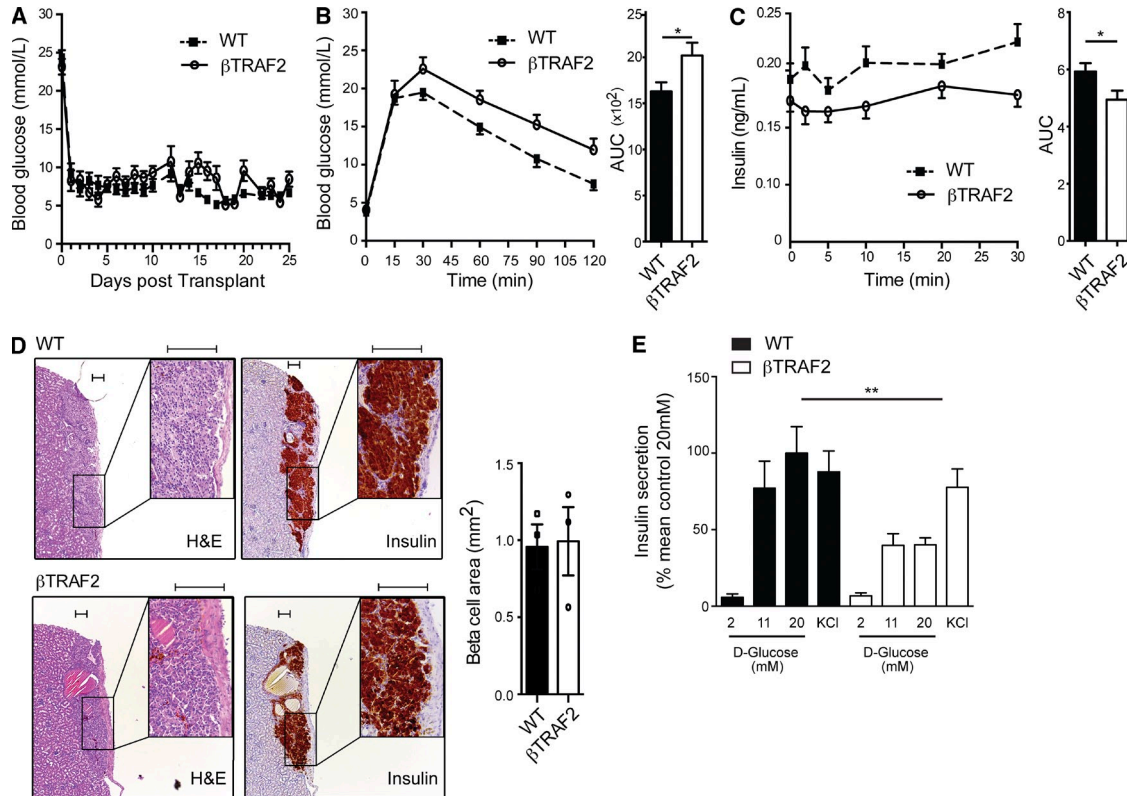
Figure 4. Deletion of TRAF2 causes impaired glucose tolerance independent of Cre expression in the hypothalamus. (A) Non-fasted blood glucose levels in STZ-treated C57BL/6 recipients transplanted with 150 IEQs of WT (dotted line) and βTRAF2 (solid line) islets were determined. Data are representative of three independent mouse cohorts, in which 15 TRAF2$_{loxP/loxP}$ (WT), 10 RI Cre (WT), and 14 βTRAF2 islet transplant recipients were tested. (B) Blood glucose and AUC were assessed in 8 TRAF2$_{loxP/loxP}$ (WT), 4 RI Cre (WT), and 10 βTRAF2 islet transplant recipients after i.p. injection of D-glucose at day 11 after transplant. Data are representative of three independent mouse cohorts tested. *, P < 0.05. (C) Insulin levels and AUC were assessed in 6 TRAF2$_{loxP/loxP}$ (WT), 4 RI Cre (WT), and 10 βTRAF2 islet transplant recipients after i.v. injection of D-glucose at day 21 after transplant. Data are representative of three independent mouse cohorts tested. *, P < 0.05. (D) H&E staining and insulin immunohistochemistry of WT and βTRAF2 islet grafts are shown. Graft β cell area was determined for three WT and three βTRAF2 islet grafts by quantification of insulin-positive area in continuous serial graft sections. A representative image for each condition is shown. Boxed insets represent magnified area. Differences in graft area are not significant (P > 0.05). Bar, 100 μm. (E) In vitro GSIS in 2, 11, and 20 mM D-glucose and in KCl conditions in WT and βTRAF2 mouse islets was measured. Data are mean and SEM derived from six independent islet isolates for each group, and are representative of two independent experiments. **, P < 0.01. All data are represented as mean ± SEM; p-values were determined using Student's *t* test.

Ex vivo glucose–stimulated insulin secretion is diminished in βTRAF2 islets

In a second approach to establish the β cell–intrinsic defect, we challenged βTRAF2 islets in a GSIS assay. βTRAF2 islets exhibited normal basal insulin output at a glucose concentration of 2 mM (Fig. 4 E). However, when challenged with 20 mM glucose, βTRAF2 islets exhibited a 50% decrease in GSIS compared with WT islets. KCl, which induces membrane depolarization to trigger insulin secretion independent of glucose, provoked a normal insulin secretory response in βTRAF2 islets, indicating that insulin content and secretory machinery were intact in these NIK-activated islets. Collectively, the in vivo transplant and GSIS data demonstrate that the metabolic defect observed for βTRAF2 mice is β cell intrinsic.

Destabilizing the TRAF2–TRAF3–BIRC2/3 E3 ligase complex results in impaired β cell function

The β cell secretory defect in βTRAF2 mice suggests that β cell–intrinsic NIK activation results in impaired β cell function. A potential caveat to this interpretation is that TRAF2 is also necessary for molecular control over the canonical NF-κB and JNK/activator protein 1 (AP-1) signaling pathways (Yeh et al., 1997). While TRAF2 and TRAF3 are both required to suppress NIK activity, TRAF3 differs from TRAF2 as it is not involved in NF-κB and JNK/AP-1 signaling downstream of TNFR family members (Vallabhapurapu et al., 2008). Therefore, we examined NIK activation and β cell function in β cell–specific TRAF3 knockout (βTRAF3) mice. βTRAF3 islets showed reduced mRNA and protein levels of TRAF3 compared with WT islets (Fig. 5, A and B). TRAF3-deficient islets

Figure 5. Destabilization of the TRAF2–TRAF3–BIRC2/3 E3 ligase complex results in impaired β cell function. (A) TRAF3 protein levels in WT and βTRAF3 islets from one WT and one βTRAF3 mouse were assessed by immunoblotting. A representative of three independent islet isolates tested per genotype is shown. Histogram data depict mean and SEM cumulative densitometry relative to β-actin of the three independent experiments. (B) Relative expression of islet TRAF3 mRNA in six WT and three βTRAF3 islet isolates was determined by RT-PCR. Data are representative of two independent experiments. ***, P < 0.001. (C) Protein levels of NIK, IKKα/β phosphorylation, IκBα, p100 to p52 processing, and RelB in one nonstimulated WT and one βTRAF3 islet isolate were assessed by immunoblotting. A representative of three independent experiments is shown. Histogram data depict cumulative densitometry relative to β-actin of the three independent experiments. (D) Non-fasted blood glucose levels were determined in 20 TRAF3$_{loxP/loxP}$ (WT) and

showed constitutive, cell-intrinsic hyperaccumulation of NIK, higher levels of phospho-IKKα, an increased p52 to p100 ratio and increased RelB levels (Fig. 5 C). Canonical NF-κB and JNK signaling in response to TNF, however, was normal in pancreatic islets lacking TRAF3 (unpublished data), as has been described in other cell types (Gardam et al., 2011).

Chow-fed βTRAF3 mice exhibited normal weight increase, normal glucose tolerance at 8 wk of age (not depicted), and normal nonfasted blood glucose levels (Fig. 5 D), but they displayed mildly decreased glucose tolerance and insulin secretion at 16 wk of age compared with WT mice (Fig. 5, E and F). In a DIO model, βTRAF3 mice presented with abnormally high nonfasted blood glucose levels (Fig. 5 D), impaired glucose tolerance (Fig. 5 G), and a reduction in GSIS in vivo compared with WT mice (Fig. 5 H). Analysis of total pancreatic insulin content and β cell mass revealed that DIO βTRAF3 mice exhibited increased pancreatic insulin content compared with WT mice due to an increase in their β cell area (Fig. 5, I and J). Further to this, βTRAF3 islets showed reduced GSIS ex vivo but a normal insulin secretory response to KCl (Fig. 5 K). Thus, βTRAF3 mice phenocopy βTRAF2 mice with β cell–intrinsic NIK hyperactivation and impaired β cell function.

Loss of BIRC proteins results in impaired β cell function

The key role of TRAF2 and TRAF3 in regulation of NIK is the recruitment and directed control of the E3 ligase activity of BIRC proteins toward NIK. As MV1-induced NIK activation occurs through BIRC2 and BIRC3 degradation, we hypothesized genetic ablation of BIRC2 and BIRC3 in β cells would trigger a β cell defect. Mice that lack both BIRC2 and BIRC3 in their β cells (βBIRC2/3) exhibit islet-intrinsic NIK hyperactivation, as indicated by increased p100 processing (Fig. 6 A) with impaired glucose tolerance and reduced insulin secretion in a DIO model (Fig. 6, B and C). These data demonstrate that all components of the TRAF2–TRAF3–BIRC2–BIRC3 E3 ligase complex are required to provide the β cell protective circuit that reigns in the deleterious activation of NIK, which suggests that firm regulation of NIK in β cells is essential to control glucose sensing and insulin

secretion. Further, these data demonstrate that NIK activation precipitates β cell failure in a DIO model.

Expression profiling of βTRAF2 and βTRAF3 islets reveals a diabetes gene signature

To determine the molecular basis for islet dysfunction, we determined genes that were differentially expressed in both βTRAF2 and βTRAF3 islets compared with WT islets using microarray analysis. We identified 26 differentially expressed genes common to the chow-fed βTRAF2 and βTRAF3 islets and 35 differentially expressed genes common to the DIO βTRAF2 and βTRAF3 islets compared with respective WT controls (Fig. 7 A). The 15 most differentially expressed genes within chow and DIO βTRAF2 and βTRAF3 islets comparing logarithmic fold change (logFC) and their function are listed in Table 1 and Table S1. Additionally, nine differentially expressed genes overlapped between the chow and DIO βTRAF2 and βTRAF3 islets (Table 1, top six most differentially expressed genes highlighted in bold). The majority of the differentially expressed genes were up-regulated in βTRAF2 and βTRAF3 islets. This indicates that NIK and the noncanonical NF-κB pathway activate rather than repress a select transcriptional program in pancreatic β cells. The up-regulation of *Tph1*, *Lrrc55*, *Hcn1*, *Tnfrsf11b*, *Rasgrp1*, *Grem2*, and *Pde7b* in βTRAF2 and βTRAF3 islets was validated by RT-PCR in a series of independent experiments (Fig. 7 B). Gene ontology analysis highlighted regulators of growth and proliferation, metabolic genes, potassium channel components, and vesicle-associated genes, many of which are associated with diabetes in animal models (Table 2). Significantly, many of the differentially expressed genes have been identified in human studies such as GWAS, linking genes such as *Bcat1* (Grimm et al., 2003; Rampersaud et al., 2007; Keller et al., 2008; Chen et al., 2013), *Gbp4* (Westra et al., 2013), *Igfbp5* (Jehle et al., 1998; Ambra et al., 2014), *Kcnj5* (Li et al., 2012; Cnop et al., 2014; Dayeh et al., 2014), *Matn2* (Ambra et al., 2014; Cnop et al., 2014), *Rerg*, *Rph3a*, *Slca13*, and *Pde7b* (Dayeh et al., 2014), *Sftpd* (Ortega et al., 2013), *Rasgrp1* (Qu et al., 2009; Taneera et al., 2012; Li et al., 2013), or *Tnfrsf11b* (Olesen et al., 2005; Bradfield et al., 2011; Cnop et al., 2014) to type 1

---

12 βTRAF3 chow-fed mice (8 wk old; n.s.); in 20 TRAF3$_{loxP/loxP}$ (WT) and 10 βTRAF3 chow-fed mice at 16 wk old (n.s.); and in 15 TRAF3$_{loxP/loxP}$ (WT) and 12 βTRAF3 HFD-fed mice (16 wk old). *, P < 0.05. Data are representative of three independent mouse cohorts tested. (E) Blood glucose levels were measured in 20 TRAF3$_{loxP/loxP}$ (WT) and 10 βTRAF3 chow-fed mice (16 wk old) after i.p. injection of D-glucose (WT, dotted line; βTRAF3, solid line). Data are representative of three independent mouse cohorts tested. ***, P < 0.001. (F) Insulin levels were measured in six TRAF3$_{loxP/loxP}$ (WT) and six βTRAF3 chow-fed mice (16 wk old) after i.v. injection of D-glucose (WT: dotted line; βTRAF3: solid line). Data are representative of three independent mouse cohorts tested. *, P < 0.05 at 20 min after injection. (G) Blood glucose levels were measured in 15 TRAF3$_{loxP/loxP}$ (WT), 5 RI Cre (WT) and 12 βTRAF3 chow-fed mice (16 wk old) after i.p. injection of D-glucose (WT, dotted line; βTRAF3, solid line). Data are representative of three independent mouse cohorts tested. ***, P < 0.001. (H) Insulin levels were measured in 10 TRAF3$_{loxP/loxP}$ (WT), 5 RI Cre, and 8 βTRAF3 HFD-fed mice (16 wk old) after i.v. injection of D-glucose (WT, dotted line; βTRAF3, solid line). Data are representative of three independent mouse cohorts tested. *, P < 0.05. (I) Pancreatic insulin content in HFD-fed WT and βTRAF3 mice was determined. The data are mean and SEM derived from five mice per group (n.s.; P = 0.072). (J) Total β cell area was determined for HFD-fed WT and βTRAF3 mice by quantification of insulin-positive area in serial graft sections as a percentage of total pancreatic exocrine tissue. The data are mean and SEM derived from three mice per group. *, P < 0.05. (K) In vitro GSIS in 2, 11, and 20 mM D-glucose. KCl conditions in WT and βTRAF3 mouse islets were measured. Data are mean and SEM derived from six independent islet isolates for each group and are representative of two independent experiments. *, P < 0.05. All data are represented as mean ± SEM; p-values were determined using Student's t test.
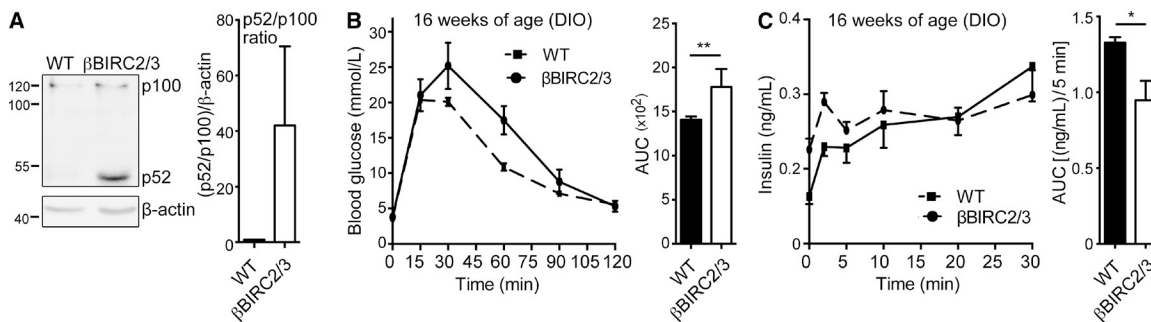
Figure 6. Genetic ablation of BIRC2 and 3 phenocopies βTRAF2 and βTRAF3 mice. (A) Protein levels of p100 to p52 processing in one WT and one βBIRC2/3 islet isolate were assessed by immunoblotting. A representative of three independent experiments is shown. Histogram data depicts cumulative densitometry relative to β-actin of the three independent experiments. (B) Blood glucose and AUC were measured in 20 WT and 6 βBIRC2/3 HFD-fed mice (16 wk old) after i.p. injection of D-glucose. Data are representative of three independent mouse cohorts tested. **, $P < 0.01$. (C) Insulin levels and AUC were measured in six WT and six βBIRC2/3 HFD-fed mice (16 wk old) after i.v. injection of D-glucose. Data are representative of three independent mouse cohorts tested. *, $P < 0.05$. All data are represented as mean ± SEM; p-values were determined using Student's t test.

and type 2 diabetes. These data identify NIK as a critical new β cell–intrinsic signaling node in diabetes integrating a transcriptional network that controls glucose homeostasis.

DISCUSSION

We have identified NIK as a novel mechanism of β cell dysfunction in obesity. Acute NIK activation using a pharmacological approach disrupts glucose homeostasis in a zebrafish model, and induces β cell dysfunction in mouse islets, but also in human islets, highlighting the importance of the NIK pathway in human islet physiology as a negative regulator of β cell function. As we have demonstrated, pancreatic β cells in a model of obesity and glucose intolerance present with β cell–intrinsic NIK activation and a decrease in β cell insulin secretory capacity. We could demonstrate that NIK was induced by inflammatory cytokines TNF and RANKL in pancreatic mouse islets. Both cytokines constitute good candidates

as NIK activators in a DIO mouse model and in human obesity. Both RANKL and TNF levels are elevated in mouse models of obesity and in T2D subjects (Hotamisligil et al., 1995; Kiechl et al., 2013). Blockade of TNF or RANKL improved glucose tolerance in mouse models of obesity (Uysal et al., 1997; Kiechl et al., 2013). Further, TNF inhibition has been shown to alleviate the metabolic syndrome in several human studies (Bernstein et al., 2006; Marra et al., 2007; Campanati et al., 2013).

Our data furthers studies showing that diet-induced obesity induces NIK in peripheral insulin-dependent tissues such as liver (Sheng et al., 2012) and muscle (Choudhary et al., 2011). Further evidence for a crucial involvement of NIK in whole body glucose homeostasis comes from studies of NIK knockout mice, which are hypoglycemic and exhibit improved glucose tolerance on a chow diet (Sheng et al., 2012). Accumulation of NIK is associated with decreased glucose uptake

Figure 7. Differentially regulated genes and expression validation by RT–PCR in βTRAF2 and βTRAF3 islets. (A) Venn diagram of the number of differentially regulated genes in βTRAF2 chow, βTRAF3 chow, βTRAF2 DIO, and βTRAF3 DIO mice compared with respective WT controls is shown. (B) A validation of gene microarray results was assessed by RT-PCR in βTRAF2 and βTRAF3 islets. The expression levels of *Tph1*, *Lrrc55*, *Hcn1*, *Tnfrsf11b* (OPG), *Rasgrp1*, *Grem2*, and *Pde7b* were examined in five βTRAF2 and five βTRAF3 islet isolates and are presented as a fold change relative to three TRAF2$_{loxP/loxP}$ and three TRAF3$_{loxP/loxP}$ (WT) islet isolates. Data are representative of two independent experiments. **, $P < 0.01$; ***, $P < 0.001$; ****, $P < 0.0001$. Data are represented as mean ± SEM; p-values were determined using Student's t test.

Table 1. Top 15 most highly differentially expressed genes in βTRAF2 and βTRAF3 islets (chow and DIO)

Gene[a]	Log FC[b]				Associated function[c]
	βTRAF2 chow	βTRAF3 chow	βTRAF2 DIO	βTRAF3 DIO	
Tph1 (tryptophan hydroxylase 1)	–	–	6.88	6.33	aromatic amino acid family metabolic process, bone remodeling, neuron projection, serotonin synthesis
Lrrc55 (leucine rich repeat containing 55)	3.78	2.90	5.00	5.04	potassium ion transport, BK channel auxiliary subunit
Sftpd (surfactant associated protein D)	3.12	2.28	4.07	3.15	phospholipid homeostasis, regulation of phagocytosis, LPS binding
Gbp8 (guanylate-binding protein 8)	3.16	–	3.59	3.36	large IFN-γ–induced GTPase
Syt10 (synaptotagmin X)	3.20	–	3.53	3.24	regulation of Ca^{2+}-dependent exocytosis, cytoplasmic vesicle
Crispld2 (cysteine-rich secretory protein LCCL domain containing 2)	3.36	3.33	–	2.68	extracellular matrix (ECM) component, heparin binding, LPS binding, vesicle transport
Hcn1 (hyper-polarization-activated, cyclic nucleotide-gated K^+ 1)	2.75	2.40	3.36	3.24	potassium ion transport; voltage-gated potassium channel, sensitivity to cAMP
Fbxw24 (F-box and WD-40 domain protein 24)	2.91	1.82	3.48	2.99	protein coding gene, unknown function
Tnfrsf11b (tumor necrosis factor receptor superfamily, member 11b)	–	–	3.20	3.19	osteoprotegerin (OPG), ECM organisation, regulation of differentiation, negative regulation of bone resorption, decoy receptor for RANKL
Matn2 (matrilin 2)	–	–	3.42	2.92	ECM, formation of filamentous networks, neuron cell migration,Ca^{2+}-binding,
Rerg (RAS-like, estrogen-regulated, growth-inhibitor)	2.13	1.56	3.30	3.04	RAS superfamily of GTPases, negative regulator of cell growth/proliferation
Rasgrp1 (RAS guanyl releasing protein 1)	3.16	3.07	–	2.93	GEF activity: activation of Ras and Rho GTPases, Ca^{2+} binding
Fmo1 (flavin containing monooxygenase 1)	–	–	3.16	2.55	drug metabolic process; oxidation-reduction process; NADPH oxidation; organic acid metabolic process
Grem2 (gremlin 2 homolog, cysteine knot superfamily (*Xenopus laevis*))	2.19	1.49	2.54	2.28	regulator of osteoblast differentiation and osteogenesis; cytokine, heparin binding, negative regulation of BMP signaling pathway
Gbp4 (guanylate binding protein 4)	2.29	2.44			large IFN-γ–induced GTPase negative regulation of protein ubiquitination

[a]Gene symbol and gene name.
[b]Log fold change of differential gene expression in chow and DIO βTRAF2 and βTRAF3 islets.
[c]Associated gene function according to DAVID Bioinformatics Database and Mouse Genome Database (MGD) at http://www.informatics.jax.org (September 2014).

in muscle (Choudhary et al., 2011) and increased hepatic glucose output by the liver (Sheng et al., 2012). Thus, NIK is emerging as a global molecular factor in obesity, therefore, these data highlight the possibility of systemic NIK inhibition as a potential therapeutic target to reduce hepatic glucose production and improve muscle uptake of glucose, while simultaneously preserving β cell function.

As we showed for pancreatic islets in diet-induced obesity, NIK levels are increased in the livers of genetically (*db/db*) and diet-induced obese mice (Sheng et al., 2012). Hepatocyte-specific NIK overexpression increased hepatic glucose output, presumably by phosphorylation and concomitant elevation and

activation of the transcription factor cAMP response element–binding (CREB) levels, which stimulates gluconeogenesis. This process is controlled by cAMP-dependent PKA phosphorylating and activating CREB. We identified *Pde7b* as a highly expressed gene in islets with constitutively activated NIK (βTRAF2 and βTRAF3 islets). *Pde7b*, which encodes for phosphodiesterase 7b (PDE7B), is involved in the conversion of cAMP to AMP, thereby decreasing cAMP secondary messenger activity (Hetman et al., 2000). cAMP regulates glucose sensing and insulin secretion in pancreatic β cells, through both PKA-dependent and–independent mechanisms (Ämmalä et al., 1994; Leclerc and Rutter, 2004). Significantly,

Table 2. Gene ontology and diabetes association of differentially expressed genes in βTRAF2 and βTRAF3 islets (chow and DIO)

	chow	DIO
Gene ontology[a]		
Regulation of cell growth, proliferation, apoptosis	*Adora1, Bcat1, Gfra3, Grem2, Rasgrp1, Rerg, Sftpd, Socs2*	*Cish, Fmo1, Igfbp5, Ngfr, Prok1, Tph1, Tnfrsf11b*
Metabolic processes	*Adora1, Bcat1, Grem2, Ogdhl, Slca13, Wipi1*	*Fmo1, Ivd, Pde7b, Tph1, Srbd1*
Potassium channel component	*Hcn1, Kcnk10, Lrrcc55*	*Hcn1, Kcnj5*
GPCR or GTPase related	*Adora1, Gbp4, Gbp10, Gpr126, Gpr182, Penk, Rasgrp1*	*Cish, Gbp8, Gpr110, Kcnj5, Rph3a*
Vesicle-associated	*Crispld2, Krtap13-1, Rasgrp1, Wipi1*	*Rph3a, Syt10, Tmem2*
Diabetes association[b]		
associated with type 1 diabetic phenotype in mouse models	*Adora1, Bcat1, Gbp4, Gbp10, Hcn1, Rasgrp1*	*Fmo1, Ngfr, Tnfrsf11b*
associated with type 2 diabetic phenotype in mouse models	*Adora1, Bcat1, Gfra3, Gpr126, Hcn1, Kcnk10, Penk, Rasgrp1, Rerg, Sftpd, Socs2, Tnfrsf9, Wipi1*	*B3galnt1, B3galt1, Cish, Cym, Fmo1, Igfbp5, Kcnj5, Ngfr, Tnfrsf11b*
associated with T1D in humans	*Gbp4, Rasgrp1*	*Igfbp5, Tnfrsf11b*
associated with T2D in humans	*Bcat1, Rasgrp1, Sftpd*	*Adarb2, Igfbp5, Ivd, Kcnj5, Pde7b, Rerg, Rph3a, Slca13, Tnfrsf11b*

[a]Genes grouped by associated biological function according to DAVID Bioinformatics Database.
[b]Genes associated with T1D and/or T2D in humans; genes associated with a diabetic phenotype in mouse models.

Pde7b and *Traf2* were both recently shown to be differentially methylated in a genome-wide analysis of human T2D pancreatic islets (Dayeh et al., 2014). *Pde7b* was found to be differentially expressed in human T2D pancreatic islets as assessed by RT-PCR, and its overexpression caused a reduction in glucose-stimulated insulin secretion in vitro (Dayeh et al., 2014). This suggests that overactivation of NIK may provide a direct link between regulation of cAMP levels and CREB activity, both in liver and in islets.

Inflammation has emerged as a key factor in the pathogenesis of the metabolic syndrome acting at the level of muscle and liver to induce insulin resistance, at adipocytes to drive elaboration of cytokines, and at the level of the β cell. Key signaling pathways include the JNK and canonical NF-κB pathways. Here, we demonstrate NIK levels are elevated in pancreatic islets isolated from diet-induced obese mice, which exhibited decreased insulin secretory capacity. Further, several genetic mouse models of constitutive β cell–intrinsic NIK activation present impaired glucose-stimulated insulin secretion in diet-induced obesity. Thus, NIK acts as a critical signaling node that regulates a transcriptional network to control glucose homeostasis. NIK activation in obesity is a feature of pancreatic β cells, liver and muscle providing a tissue-spanning mechanistic understanding of the global effects of obesity in the metabolic syndrome.

MATERIALS AND METHODS

Mouse strains. C57BL/6 mice were sourced from Australian BioResource (Mossvale, NSW, Australia). TRAF2loxP/loxP, TRAF3loxP/loxP (C57BL/6 background; gift from R. Brink, Garvan Institute, NSW, Australia) and Birc3−/− mice containing Birc2loxP/loxP (C57BL/6 background; gift from D. Vaux, Walter and Eliza Hall Institute, VIC, Australia) were crossed with RIP-Cre mice (Cre driven by the rat insulin 2 promoter; Tg[Ins2-cre]25Mgn/J, C57BL/6 background; The Jackson Laboratory) to generate β cell–specific knockout mice (βTRAF2, βTRAF3, and βBIRC2/3).

Zebrafish studies. WT zebrafish larvae were injected pericardially at 6 d after fertilization with 2 nl of 10 mM MV1 in 10% DMSO or 10% DMSO as described (Hesselson et al., 2009). Free glucose levels were analyzed 6 h after injection using a fluorescent glucose assay kit (Biovision; Jurczyk et al., 2011).

In vivo studies. For islet transplantation, 150 hand-counted primary islet equivalents isolated from male and female donor mice were transplanted into syngeneic diabetic male C57BL/6 recipients as previously described (Grey et al., 2003). Mice in the DIO model were fed a diet providing 45% calories from fat (lard/safflower oil) ad libitum. Glucose tolerance tests (i.p. 2 g/kg and i.v. 1 g/kg body weight) after a 16-h fast were performed on female βTRAF2, βTRAF3, and βBIRC2/3 mice and respective floxed and RIP Cre controls mice as previously described (Cantley et al., 2013). Blood samples for insulin ELISA (mouse ultra-sensitive kit; Crystal Chem) were collected using 5-µl micro-capillary tubes (Drummond microcaps; Sigma-Aldrich). Insulin secretory capacity was determined by normalizing insulin levels or insulin secretion measured by AUC to total β cell area. Islets were isolated as previously described (Zammit et al., 2013), from male and female donors for GSIS, RNA extraction, and Western blot protein extraction. In vivo mouse physiology experiments comprise data from at least three independent cohorts.

Analysis of TRAF2 and TRAF3 mRNA expression in isolated islets. Isolated mRNA (QIAschredder, RNEasy Plus Mini kit; QIAGEN) was reverse transcribed (Quantitect Reverse Transcription kit; QIAGEN). mRNA expression was determined by Real Time-PCRs using FastStart SYBR Green Master Mix (Roche). PCR reactions were performed with the following primers and normalized to the house-keeping gene Cyclophillin A (CpH, sense 5′-TGGACCAAACACAAACGGTTCC-3′ and antisense 5′-ACATTGCGAGCAGATGGGGTAG-3′; TRAF2, sense 5′-TCTGCCTGACC-AGCATCCTC-3′ and antisense 5′-AATGCCTTCTTCATACAGGCC-TTC-3′; TRAF3, sense 5′-CAGCGTGCCAAGAAAGCATC-3′ and antisense 5′-CGCACAACCTCTGCCTTCAT-3′). Initial denaturation was performed

at 95°C for 10 s, followed by a three step cycle consisting of 95°C for 15 s (4.8°C/s, denaturation), 63°C for 30 s (2.5°C/s, annealing), and 72°C for 30 s (4.8°C/s, elongation). A melt-curve was performed after finalization of 45 cycles at 95°C for 2 min, 40°C for 3 min, and gradual increase to 95°C with 25 acquisitions/°C.

Assessment of signaling pathway activation. Protein was extracted from islets or cell lines using a detergent-based lysis buffer. 30–40 µg of protein per well were separated on an SDS-PAGE and protein levels were determined by Western Blot analysis using the following antibodies (expected protein size [kD] is indicated): TRAF2 (C-20; 50 kD), TRAF3 (H-122; 65 kD; Santa Cruz Biotechnology Inc.), IκBα (39 kD), NIK (125 kD), phospho-IKKα/β (85/87 kD), p100/p52 (120 & 52kD), RelB (70 kD; Cell Signaling Technology), β-actin (42 kD; Sigma-Aldrich), anti–rabbit IgG (horseradish peroxidase-conjugated; Thermo Fisher Scientific), and anti–mouse IgG (and horseradish peroxidase-conjugated; Thermo Fisher Scientific). Signals were visualized using an enhanced chemiluminescence detection kit (Amersham Pharmacia Biotech). Western blot signals were quantified using the ImageJ (NIH) histogram function. Subsequently, the band intensity was normalized to relative protein concentration using β actin as a reference.

Immunohistochemistry and β cell area determination. Tissues were fixed in 10% buffered formalin and 5-µm paraffin sections were stained with hematoxylin-eosin. Serial consecutive sections in 100-µm intervals were stained for insulin (polyclonal anti–rabbit; Cell Signaling Technology) and counter-stained with hematoxylin. β cell area was assessed by determining total insulin-positive area (ImageJ).

GSIS. Three human pancreatic islet isolates were prepared at the St. Vincent's Hospital Centre for Islet Isolation (Melbourne, Australia) from heart-beating deceased donors. GSIS was determined for islets ex vivo as described (Cantley et al., 2013).

Whole pancreas insulin content. To determine whole pancreas insulin content, pancreata were collected and immediately immersed in ice-cold acidified ethanol. The tissue was homogenized with a tissue homogenizer (Heidolph Silent Crusher M) and total pancreatic insulin content was determined by insulin ELISA (mouse ultra-sensitive kit; Crystal Chem).

Synthesis and purification of the MV1 compound. The synthetic routes of MV1 production are available upon request.

Microarray. The quality of mRNA isolated from primary islets was evaluated by using an Agilent 2100 Bioanalyzer (Agilent Technologies). Samples were run in triplicates on a MoGene2.0 (GeneChip Mouse Gene 2.0 ST Array, Affymetrix) at the Ramaciotti Center (University of New South Wales, Australia). Raw data were deposited in the Gene Expression Omnibus database: accession no. GSE68317.

Statistical analysis. Statistical analysis was performed using an unpaired two-tailed Students t test using Prism software (GraphPad Inc.). Error bars in all figures represent SEM as specified.

Study approval. Animal studies were approved by the Garvan/St Vincent's Animal Ethics Committee (AEC) fulfilling all the requirements of the NH&MRC and the NSW State Government. All procedures performed complied with the Australian Code of Practice for Care and Use of Animals for Scientific Purposes. This project was reviewed and approved by the St Vincent's Hospital (Melbourne, Australia) Human Research Ethics Committee: HREC-A 011/04.

Online supplemental material. Table S1 is a complete list of differentially expressed genes overlapping βTRAF2 and βTRAF3 islets (chow and DIO). Online supplemental material is available at http://www.jem.org/cgi/content/full/jem.20150218/DC1.

Author contributions: E.K. Malle and S.T. Grey designed and led the study. E.K. Malle, N.W. Zammit, S.N. Walters, and J. Cantley conducted mouse experiments and analyzed data. J. Wu wrote code and analyzed microarray data. T. Loudovaris conducted experiments with human islets. R. Brink provided critical resources and expertise. S.R. McAlpine and Y.C. Koay designed and synthesized MV1. D. Hesselson designed and conducted zebrafish experiments. E.K. Malle, S.R. McAlpine, D. Hesselson, J. Cantley, and S.T. Grey critically assessed data and provided intellectual input. E.K. Malle and S.T. Grey co-wrote the manuscript.

REFERENCES

Ambra, R., S. Manca, M.C. Palumbo, G. Leoni, L. Natarelli, A. De Marco, A. Consoli, A. Pandolfi, and F. Virgili. 2014. Transcriptome analysis of human primary endothelial cells (HUVEC) from umbilical cords of gestational diabetic mothers reveals candidate sites for an epigenetic modulation of specific gene expression. *Genomics.* 103:337–348. http://dx.doi.org/10.1016/j.ygeno.2014.03.003

Ammälä, C., L. Eliasson, K. Bokvist, P.O. Berggren, R.E. Honkanen, A. Sjöholm, and P. Rorsman. 1994. Activation of protein kinases and inhibition of protein phosphatases play a central role in the regulation of exocytosis in mouse pancreatic beta cells. *Proc. Natl. Acad. Sci. USA.* 91:4343–4347. http://dx.doi.org/10.1073/pnas.91.10.4343

Bernstein, L.E., J. Berry, S. Kim, B. Canavan, and S.K. Grinspoon. 2006. Effects of etanercept in patients with the metabolic syndrome. *Arch. Intern. Med.* 166:902–908. http://dx.doi.org/10.1001/archinte.166.8.902

Bonizzi, G., M. Bebien, D.C. Otero, K.E. Johnson-Vroom, Y. Cao, D. Vu, A.G. Jegga, B.J. Aronow, G. Ghosh, R.C. Rickert, and M. Karin. 2004. Activation of IKKalpha target genes depends on recognition of specific kappaB binding sites by RelB:p52 dimers. *EMBO J.* 23:4202–4210. http://dx.doi.org/10.1038/sj.emboj.7600391

Bradfield, J.P., H.Q. Qu, K. Wang, H. Zhang, P.M. Sleiman, C.E. Kim, F.D. Mentch, H. Qiu, J.T. Glessner, K.A. Thomas, et al. 2011. A genome-wide meta-analysis of six type 1 diabetes cohorts identifies multiple associated loci. *PLoS Genet.* 7:e1002293. http://dx.doi.org/10.1371/journal.pgen.1002293

Butler, A.E., J. Janson, S. Bonner-Weir, R. Ritzel, R.A. Rizza, and P.C. Butler. 2003. Beta-cell deficit and increased beta-cell apoptosis in humans with type 2 diabetes. *Diabetes.* 52:102–110. http://dx.doi.org/10.2337/diabetes.52.1.102

Campanati, A., G. Ganzetti, A. Di Sario, A. Damiani, L. Sandroni, L. Rosa, A. Benedetti, and A. Offidani. 2013. The effect of etanercept on hepatic fibrosis risk in patients with non-alcoholic fatty liver disease, metabolic syndrome, and psoriasis. *J. Gastroenterol.* 48:839–846. http://dx.doi.org/10.1007/s00535-012-0678-9

Cantley, J., S.N. Walters, M.H. Jung, A. Weinberg, M.J. Cowley, T.P. Whitworth, W. Kaplan, W.J. Hawthorne, P.J. O'Connell, G. Weir, and S.T. Grey. 2013. A preexistent hypoxic gene signature predicts impaired islet graft function and glucose homeostasis. *Cell Transplant.* 22:2147–2159. http://dx.doi.org/10.3727/096368912X658728

Chen, J., Y. Meng, J. Zhou, M. Zhuo, F. Ling, Y. Zhang, H. Du, and X. Wang. 2013. Identifying candidate genes for Type 2 Diabetes Mellitus and obesity through gene expression profiling in multiple tissues or cells. *J Diabetes Res.* 2013:970435. http://dx.doi.org/10.1155/2013/970435

Chiang, S.H., M. Bazuine, C.N. Lumeng, L.M. Geletka, J. Mowers, N.M. White, J.T. Ma, J. Zhou, N. Qi, D. Westcott, et al. 2009. The protein kinase IKKepsilon regulates energy balance in obese mice. *Cell*. 138:961–975. http://dx.doi.org/10.1016/j.cell.2009.06.046

Choudhary, S., S. Sinha, Y. Zhao, S. Banerjee, P. Sathyanarayana, S. Shahani, V. Sherman, R.G. Tilton, and M. Bajaj. 2011. NF-kappaB-inducing kinase (NIK) mediates skeletal muscle insulin resistance: blockade by adiponectin. *Endocrinology*. 152:3622–3627. http://dx.doi.org/10.1210/en.2011-1343

Cnop, M., B. Abdulkarim, G. Bottu, D.A. Cunha, M. Igoillo-Esteve, M. Masini, J.V. Turatsinze, T. Griebel, O. Villate, I. Santin, et al. 2014. RNA sequencing identifies dysregulation of the human pancreatic islet transcriptome by the saturated fatty acid palmitate. *Diabetes*. 63:1978–1993. http://dx.doi.org/10.2337/db13-1383

Dayeh, T., P. Volkov, S. Salö, E. Hall, E. Nilsson, A.H. Olsson, C.L. Kirkpatrick, C.B. Wollheim, L. Eliasson, T. Rönn, et al. 2014. Genome-wide DNA methylation analysis of human pancreatic islets from type 2 diabetic and non-diabetic donors identifies candidate genes that influence insulin secretion. *PLoS Genet*. 10:e1004160. http://dx.doi.org/10.1371/journal.pgen.1004160

Donath, M.Y., D.J. Gross, E. Cerasi, and N. Kaiser. 1999. Hyperglycemia-induced beta-cell apoptosis in pancreatic islets of Psammomys obesus during development of diabetes. *Diabetes*. 48:738–744. http://dx.doi.org/10.2337/diabetes.48.4.738

Ferrannini, E., and A. Mari. 2014. β-Cell function in type 2 diabetes. *Metabolism*. 63:1217–1227. http://dx.doi.org/10.1016/j.metabol.2014.05.012

Florez, J.C. 2008. Newly identified loci highlight beta cell dysfunction as a key cause of type 2 diabetes: where are the insulin resistance genes? *Diabetologia*. 51:1100–1110. http://dx.doi.org/10.1007/s00125-008-1025-9

Fulda, S., and D. Vucic. 2012. Targeting IAP proteins for therapeutic intervention in cancer. *Nat. Rev. Drug Discov*. 11:109–124. http://dx.doi.org/10.1038/nrd3627

Gardam, S., F. Sierro, A. Basten, F. Mackay, and R. Brink. 2008. TRAF2 and TRAF3 signal adapters act cooperatively to control the maturation and survival signals delivered to B cells by the BAFF receptor. *Immunity*. 28:391–401. http://dx.doi.org/10.1016/j.immuni.2008.01.009

Gardam, S., V.M. Turner, H. Anderton, S. Limaye, A. Basten, F. Koentgen, D.L. Vaux, J. Silke, and R. Brink. 2011. Deletion of cIAP1 and cIAP2 in murine B lymphocytes constitutively activates cell survival pathways and inactivates the germinal center response. *Blood*. 117:4041–4051. http://dx.doi.org/10.1182/blood-2010-10-312793

Goldfine, A.B., V. Fonseca, K.A. Jablonski, Y.D. Chen, L. Tipton, M.A. Staten, S.E. Shoelson, and T. Targeting Inflammation Using Salsalate. Targeting Inflammation Using Salsalate in Type 2 Diabetes Study Team. 2013. Salicylate (salsalate) in patients with type 2 diabetes: a randomized trial. *Ann. Intern. Med*. 159:1–12. http://dx.doi.org/10.7326/0003-4819-159-1-201307020-00003

Grey, S.T., C. Longo, T. Shukri, V.I. Patel, E. Csizmadia, S. Daniel, M.B. Arvelo, V. Tchipashvili, and C. Ferran. 2003. Genetic engineering of a suboptimal islet graft with A20 preserves beta cell mass and function. *J. Immunol*. 170:6250–6256. http://dx.doi.org/10.4049/jimmunol.170.12.6250

Grimm, C.H., U.C. Rogner, and P. Avner. 2003. Lrmp and Bcat1 are candidates for the type I diabetes susceptibility locus Idd6. *Autoimmunity*. 36:241–246. http://dx.doi.org/10.1080/0891693031000141068

Guan, W., A. Pluzhnikov, N.J. Cox, and M. Boehnke. International Type 2 Diabetes Linkage Analysis Consortium. 2008. Meta-analysis of 23 type 2 diabetes linkage studies from the International Type 2 Diabetes Linkage Analysis Consortium. *Hum. Hered*. 66:35–49. http://dx.doi.org/10.1159/000114164

Hesselson, D., R.M. Anderson, M. Beinat, and D.Y. Stainier. 2009. Distinct populations of quiescent and proliferative pancreatic beta-cells identified by HOTcre mediated labeling. *Proc. Natl. Acad. Sci. USA*. 106:14896–14901. http://dx.doi.org/10.1073/pnas.0906348106

Hetman, J.M., S.H. Soderling, N.A. Glavas, and J.A. Beavo. 2000. Cloning and characterization of PDE7B, a cAMP-specific phosphodiesterase. *Proc. Natl. Acad. Sci. USA*. 97:472–476. http://dx.doi.org/10.1073/pnas.97.1.472

Hotamisligil, G.S., P. Arner, J.F. Caro, R.L. Atkinson, and B.M. Spiegelman. 1995. Increased adipose tissue expression of tumor necrosis factor-alpha in human obesity and insulin resistance. *J. Clin. Invest*. 95:2409–2415. http://dx.doi.org/10.1172/JCI117936

Hundal, R.S., K.F. Petersen, A.B. Mayerson, P.S. Randhawa, S. Inzucchi, S.E. Shoelson, and G.I. Shulman. 2002. Mechanism by which high-dose aspirin improves glucose metabolism in type 2 diabetes. *J. Clin. Invest*. 109:1321–1326. http://dx.doi.org/10.1172/JCI0214955

Jehle, P.M., D.R. Jehle, S. Mohan, and B.O. Böhm. 1998. Serum levels of insulin-like growth factor system components and relationship to bone metabolism in Type 1 and Type 2 diabetes mellitus patients. *J. Endocrinol*. 159:297–306. http://dx.doi.org/10.1677/joe.0.1590297

Jurczyk, A., N. Roy, R. Bajwa, P. Gut, K. Lipson, C. Yang, L. Covassin, W.J. Racki, A.A. Rossini, N. Phillips, et al. 2011. Dynamic glucoregulation and mammalian-like responses to metabolic and developmental disruption in zebrafish. *Gen. Comp. Endocrinol*. 170:334–345. http://dx.doi.org/10.1016/j.ygcen.2010.10.010

Keller, M.P., Y. Choi, P. Wang, D.B. Davis, M.E. Rabaglia, A.T. Oler, D.S. Stapleton, C. Argmann, K.L. Schueler, S. Edwards, et al. 2008. A gene expression network model of type 2 diabetes links cell cycle regulation in islets with diabetes susceptibility. *Genome Res*. 18:706–716. http://dx.doi.org/10.1101/gr.074914.107

Kiechl, S., J. Wittmann, A. Giaccari, M. Knoflach, P. Willeit, A. Bozec, A.R. Moschen, G. Muscogiuri, G.P. Sorice, T. Kireva, et al. 2013. Blockade of receptor activator of nuclear factor-κB (RANKL) signaling improves hepatic insulin resistance and prevents development of diabetes mellitus. *Nat. Med*. 19:358–363. http://dx.doi.org/10.1038/nm.3084

Leclerc, I., and G.A. Rutter. 2004. AMP-activated protein kinase: a new beta-cell glucose sensor?: Regulation by amino acids and calcium ions. *Diabetes*. 53:S67–S74. http://dx.doi.org/10.2337/diabetes.53.suppl_3.S67

Li, H., W. Gan, L. Lu, X. Dong, X. Han, C. Hu, Z. Yang, L. Sun, W. Bao, P. Li, et al. AGEN-T2D Consortium. 2013. A genome-wide association study identifies GRK5 and RASGRP1 as type 2 diabetes loci in Chinese Hans. *Diabetes*. 62:291–298. http://dx.doi.org/10.2337/db12-0454

Li, N.F., Y.A. Kang, D.L. Zhang, H.M. Wang, J.H. Zhang, Y.R. Hu, and J. Hong. 2012. [Association between GIRK4 gene polymorphisms and insulin resistance in Xinjiang Uygur population]. *Zhonghua Yi Xue Yi Chuan Xue Za Zhi*. 29:715–719.

Marra, M., A. Campanati, R. Testa, C. Sirolla, A.R. Bonfigli, C. Franceschi, F. Marchegiani, and A. Offidani. 2007. Effect of etanercept on insulin sensitivity in nine patients with psoriasis. *Int. J. Immunopathol. Pharmacol*. 20:731–736.

Novack, D.V., L. Yin, A. Hagen-Stapleton, R.D. Schreiber, D.V. Goeddel, F.P. Ross, and S.L. Teitelbaum. 2003. The IkappaB function of NF-kappaB2 p100 controls stimulated osteoclastogenesis. *J. Exp. Med*. 198:771–781. http://dx.doi.org/10.1084/jem.20030116

Olesen, P., T. Ledet, and L.M. Rasmussen. 2005. Arterial osteoprotegerin: increased amounts in diabetes and modifiable synthesis from vascular smooth muscle cells by insulin and TNF-alpha. *Diabetologia*. 48:561–568. http://dx.doi.org/10.1007/s00125-004-1652-8

Ortega, F.J., N. Pueyo, J.M. Moreno-Navarrete, M. Sabater, J.I. Rodriguez-Hermosa, W. Ricart, F.J. Tinahones, and J.M. Fernández-Real. 2013. The lung innate immune gene surfactant protein-D is expressed in adipose tissue and linked to obesity status. *Int. J. Obes. (Lond)*. 37:1532–1538. http://dx.doi.org/10.1038/ijo.2013.23

Ortis, F., N. Naamane, D. Flamez, L. Ladrière, F. Moore, D.A. Cunha, M.L. Colli, T. Thykjaer, K. Thorsen, T.F. Orntoft, and D.L. Eizirik. 2010. Cytokines interleukin-1beta and tumor necrosis factor-alpha regulate different transcriptional and alternative splicing networks in primary beta-cells. *Diabetes*. 59:358–374. http://dx.doi.org/10.2337/db09-1159

Peyot, M.L., E. Pepin, J. Lamontagne, M.G. Latour, B. Zarrouki, R. Lussier, M. Pineda, T.L. Jetton, S.R. Madiraju, E. Joly, and M. Prentki. 2010. Beta-cell failure in diet-induced obese mice stratified according to body weight gain: secretory dysfunction and altered islet lipid metabolism without steatosis or reduced beta-cell mass. *Diabetes*. 59:2178–2187. http://dx.doi.org/10.2337/db09-1452

Qu, H.Q., S.F.A. Grant, J.P. Bradfield, C. Kim, E. Frackelton, H. Hakonarson, and C. Polychronakos. 2009. Association of RASGRP1 with

type 1 diabetes is revealed by combined follow-up of two genome-wide studies. *J. Med. Genet.* 46:553–554. http://dx.doi.org/10.1136/jmg.2009 .067140

Rampersaud, E., C.M. Damcott, M. Fu, H. Shen, P. McArdle, X. Shi, J. Shelton, J. Yin, Y.-P.C. Chang, S.H. Ott, et al. 2007. Identification of novel candidate genes for type 2 diabetes from a genome-wide association scan in the Old Order Amish: evidence for replication from diabetes-related quantitative traits and from independent populations. *Diabetes.* 56:3053–3062. http://dx.doi.org/10.2337/db07-0457

Rauert, H., A. Wicovsky, N. Müller, D. Siegmund, V. Spindler, J. Waschke, C. Kneitz, and H. Wajant. 2010. Membrane tumor necrosis factor (TNF) induces p100 processing via TNF receptor-2 (TNFR2). *J. Biol. Chem.* 285:7394–7404. http://dx.doi.org/10.1074/jbc.M109.037341

Reilly, S.M., S.H. Chiang, S.J. Decker, L. Chang, M. Uhm, M.J. Larsen, J.R. Rubin, J. Mowers, N.M. White, I. Hochberg, et al. 2013. An inhibitor of the protein kinases TBK1 and IKK-ε improves obesity–related metabolic dysfunctions in mice. *Nat. Med.* 19:313–321. http://dx.doi .org/10.1038/nm.3082

Seth, A., D.L. Stemple, and I. Barroso. 2013. The emerging use of zebrafish to model metabolic disease. *Dis. Model. Mech.* 6:1080–1088. http:// dx.doi.org/10.1242/dmm.011346

Sheng, L., Y. Zhou, Z. Chen, D. Ren, K.W. Cho, L. Jiang, H. Shen, Y. Sasaki, and L. Rui. 2012. NF-κB–inducing kinase (NIK) promotes hyperglycemia and glucose intolerance in obesity by augmenting glucagon action. *Nat. Med.* 18:943–949. http://dx.doi.org/10.1038/nm.2756

Spranger, J., A. Kroke, M. Möhlig, K. Hoffmann, M.M. Bergmann, M. Ristow, H. Boeing, and A.F. Pfeiffer. 2003. Inflammatory cytokines and the risk to develop type 2 diabetes: results of the prospective population-based European Prospective Investigation into Cancer and Nutrition (EPIC)-Potsdam Study. *Diabetes.* 52:812–817. http://dx.doi.org/10.2337/ diabetes.52.3.812

Sun, S.-C. 2011. Non-canonical NF-κB signaling pathway. *Cell Res.* 21:71–85. http://dx.doi.org/10.1038/cr.2010.177

Taneera, J., S. Lang, A. Sharma, J. Fadista, Y. Zhou, E. Ahlqvist, A. Jonsson, V. Lyssenko, P. Vikman, O. Hansson, et al. 2012. A systems genetics approach identifies genes and pathways for type 2 diabetes in human islets. *Cell Metab.* 16:122–134. http://dx.doi.org/10.1016/j.cmet.2012.06.006

Uysal, K.T., S.M. Wiesbrock, M.W. Marino, and G.S. Hotamisligil. 1997. Protection from obesity-induced insulin resistance in mice lacking TNF-alpha function. *Nature.* 389:610–614. http://dx.doi.org/10.1038/ 39335

Vallabhapurapu, S., A. Matsuzawa, W. Zhang, P.-H. Tseng, J.J. Keats, H. Wang, D.A.A. Vignali, P.L. Bergsagel, and M. Karin. 2008. Nonredundant and complementary functions of TRAF2 and TRAF3 in a ubiquitination cascade that activates NIK-dependent alternative NF-kappaB signaling. *Nat. Immunol.* 9:1364–1370. http://dx.doi.org/10.1038/ ni.1678

Varfolomeev, E., J.W. Blankenship, S.M. Wayson, A.V. Fedorova, N. Kayagaki, P. Garg, K. Zobel, J.N. Dynek, L.O. Elliott, H.J. Wallweber, et al. 2007. IAP antagonists induce autoubiquitination of c-IAPs, NF-kappaB activation, and TNFalpha-dependent apoptosis. *Cell.* 131:669–681. http://dx.doi .org/10.1016/j.cell.2007.10.030

Verchere, C.B., D.A. D'Alessio, R.D. Palmiter, G.C. Weir, S. Bonner-Weir, D.G. Baskin, and S.E. Kahn. 1996. Islet amyloid formation associated with hyperglycemia in transgenic mice with pancreatic beta cell expression of human islet amyloid polypeptide. *Proc. Natl. Acad. Sci. USA.* 93:3492–3496. http://dx.doi.org/10.1073/pnas.93.8.3492

Westra, H.J., M.J. Peters, T. Esko, H. Yaghootkar, C. Schurmann, J. Kettunen, M.W. Christiansen, B.P. Fairfax, K. Schramm, J.E. Powell, et al. 2013. Systematic identification of trans eQTLs as putative drivers of known disease associations. *Nat. Genet.* 45:1238–1243. http://dx.doi.org/10.1038/ ng.2756

Wicksteed, B., M. Brissova, W. Yan, D.M. Opland, J.L. Plank, R.B. Reinert, L.M. Dickson, N.A. Tamarina, L.H. Philipson, A. Shostak, et al. 2010. Conditional gene targeting in mouse pancreatic β-cells: analysis of ectopic Cre transgene expression in the brain. *Diabetes.* 59:3090–3098. http:// dx.doi.org/10.2337/db10-0624

Winzell, M.S., and B. Ahrén. 2004. The high-fat diet-fed mouse: a model for studying mechanisms and treatment of impaired glucose tolerance and type 2 diabetes. *Diabetes.* 53(Suppl 3):S215–S219. http://dx.doi .org/10.2337/diabetes.53.suppl_3.S215

Xie, P., Z.J. Kraus, L.L. Stunz, Y. Liu, and G.A. Bishop. 2011. TNF receptor-associated factor 3 is required for T cell–mediated immunity and TCR/CD28 signaling. *J. Immunol.* 186:143–155. http://dx.doi.org/ 10.4049/jimmunol.1000290

Yeh, W.-C., A. Shahinian, D. Speiser, J. Kraunus, F. Billia, A. Wakeham, J.L. de la Pompa, D. Ferrick, B. Hum, N. Iscove, et al. 1997. Early lethality, functional NF-kappaB activation, and increased sensitivity to TNF-induced cell death in TRAF2-deficient mice. *Immunity.* 7:715–725. http:// dx.doi.org/10.1016/S1074-7613(00)80391-X

Yuan, M., N. Konstantopoulos, J. Lee, L. Hansen, Z.W. Li, M. Karin, and S.E. Shoelson. 2001. Reversal of obesity- and diet-induced insulin resistance with salicylates or targeted disruption of Ikkbeta. *Science.* 293:1673–1677. http://dx.doi.org/10.1126/science.1061620

Zammit, N.W., B.M. Tan, S.N. Walters, D. Liuwantara, J.E. Villanueva, E.K. Malle, and S.T. Grey. 2013. Low-dose rapamycin unmasks the protective potential of targeting intragraft NF-κB for islet transplants. *Cell Transplant.* 22:2355–2366. http://dx.doi.org/10.3727/096368912X658737

Zarnegar, B.J., Y. Wang, D.J. Mahoney, P.W. Dempsey, H.H. Cheung, J. He, T. Shiba, X. Yang, W.C. Yeh, T.W. Mak, et al. 2008. Noncanonical NF-kappaB activation requires coordinated assembly of a regulatory complex of the adaptors cIAP1, cIAP2, TRAF2 and TRAF3 and the kinase NIK. *Nat. Immunol.* 9:1371–1378. http://dx.doi.org/10.1038/ ni.1676